

Photopharmacology

International Edition: DOI: 10.1002/anie.201703890
German Edition: DOI: 10.1002/ange.201703890

A Red-Light-Activated Ruthenium-Caged NAMPT Inhibitor Remains Phototoxic in Hypoxic Cancer Cells

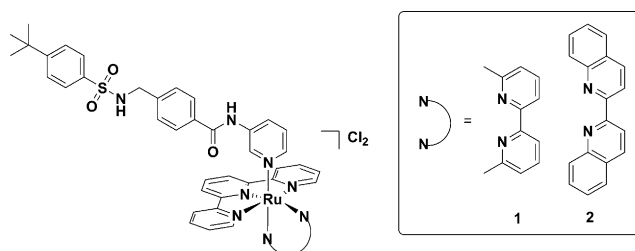
Lucien N. Lameijer, Daniël Ernst, Samantha L. Hopkins, Michael S. Meijer, Sven H. C. Askes, Sylvia E. Le Dévédec, and Sylvestre Bonnet*

Abstract: We describe two water-soluble ruthenium complexes, **[1]Cl₂** and **[2]Cl₂**, that photodissociate to release a cytotoxic nicotinamide phosphoribosyltransferase (NAMPT) inhibitor with a low dose (21 J cm⁻²) of red light in an oxygen-independent manner. Using a specific NAMPT activity assay, up to an 18-fold increase in inhibition potency was measured upon red-light activation of **[2]Cl₂**, while **[1]Cl₂** was thermally unstable. For the first time, the dark and red-light-induced cytotoxicity of these photocaged compounds could be tested under hypoxia (1% O₂). In skin (A431) and lung (A549) cancer cells, a 3- to 4-fold increase in cytotoxicity was found upon red-light irradiation for **[2]Cl₂**, whether the cells were cultured and irradiated with 1% or 21% O₂. These results demonstrate the potential of photoactivated chemotherapy for hypoxic cancer cells, in which classical photodynamic therapy, which relies on oxygen activation, is poorly efficient.

NAMPT is a key enzyme in the salvage pathway of NAD⁺ biosynthesis, and is abnormally up regulated in cancer cells.^[1] Importantly, high NAMPT expression has been associated with poor prognosis in different types of cancer, which makes NAMPT a potential therapeutic target.^[2] It has been shown that NAMPT inhibition leads to a reduction in NAD⁺ intracellular levels, which can induce apoptosis in cancer cells.^[2a,3] However, it has also been reported that targeting of NAMPT might lead to side effects such as blindness.^[4] A strategy called PhotoActivated ChemoTherapy (PACT) might solve selectivity issues.^[5] PACT consists of masking the toxicity of a drug with a caging agent that is released upon

light irradiation, together with the free drug.^[5b,6] Ruthenium polypyridyl complexes are particularly promising photocaging groups since they can be removed using visible light,^[7] whereas most organic caging groups require UV light for activation.^[8] Unlike photodynamic therapy (PDT), a clinically approved therapeutic approach that relies on the photocatalytic activation of ³O₂ into ¹O₂ by a photosensitizer,^[9] PACT is oxygen-independent,^[5b,9] which makes it a promising and complementary therapeutic strategy for addressing hypoxic tumours. However, proof of efficacy of PACT under hypoxia is still lacking.

Herein, we describe a setup using monochromatic red light on living cells under hypoxia (1%) for studying the PACT compounds **[1]Cl₂** and **[2]Cl₂** (Scheme 1). Red light is



Scheme 1. Caged STF-31 compounds **[1]Cl₂** and **[2]Cl₂**.

superior to previously reported blue- or green-light activation of PACT compounds owing to its deeper tissue penetration (0.5–1.0 cm),^[10] and can be used with higher doses without significant light-induced cytotoxicity.^[11] Two sterically hindered ruthenium photocaging scaffolds were chosen based upon earlier work by the group of Turro and Kodanko:^[12] $[\text{Ru}(\text{tpy})(\text{dmbpy})(\text{L})]^{2+}$ (tpy = 2,2',6'-terpyridine; dmbpy = 6,6'-dimethyl-2,2'-bipyridine) and $[\text{Ru}(\text{tpy})(\text{biq})(\text{L})]^{2+}$ (biq = 2,2'-biquinoline). Both types of complexes have an absorption band that extends into the red region of the spectrum,^[13] and they photodissociate when the monodentate ligand (L) is a thioether or a pyridine moiety.^[12a,14] These scaffolds were conjugated to 4-([4-(2-methyl-2-prop-1-enyl)phenyl]sulfonyl)amino)methyl-N-(3-pyridinyl)benzamide (STF-31), a known cytotoxic organic compound containing a pyridine moiety that can coordinate to ruthenium. The toxicity of STF-31 was reported to originate from inhibition of both NAMPT^[15] and GLUT1.^[16] We synthesized the two STF-31-containing compounds **[1]Cl₂** and **[2]Cl₂** (Scheme 1), demonstrated that red light can uncage STF-31, and show that this leads to efficient PACT under both normoxia (21% O₂) and hypoxia (1% O₂).

[*] L. N. Lameijer, D. Ernst, Dr. S. L. Hopkins, M. S. Meijer, Dr. S. H. C. Askes, Dr. S. Bonnet
Leiden Institute of Chemistry, Leiden University
Gorlaeus Laboratories
P.O. Box 9502, 2300 RA Leiden (The Netherlands)
E-mail: bonnet@chem.leidenuniv.nl

Dr. S. E. Le Dévédec
Leiden Academic Centre for Drug Research, Leiden University
Gorlaeus Laboratories
P.O. Box 9502, 2300 RA Leiden (The Netherlands)

Supporting information (including experimental details) and the ORCID identification number(s) for the author(s) of this article can be found under:
<https://doi.org/10.1002/anie.201703890>.

© 2017 The Authors. Published by Wiley-VCH Verlag GmbH & Co. KGaA. This is an open access article under the terms of the Creative Commons Attribution Non-Commercial License, which permits use, distribution and reproduction in any medium, provided the original work is properly cited, and is not used for commercial purposes.

Compounds **[1]Cl₂** and **[2]Cl₂** were synthesized by reacting STF-31 with the precursors [Ru(tpy)(dmbpy)(Cl)]Cl^[14] and [Ru(tpy)(biq)(Cl)]Cl, respectively (Scheme S1 in the Supporting Information). Compounds were isolated as PF₆ salts, purified over Sephadex LH-20, and converted into their chloride salt by salt metathesis to afford **[1]Cl₂** and **[2]Cl₂** as red or purple solids in 50% and 44% yield, respectively.

One of the challenges in PACT is to find the ideal balance between thermal stability and photoactivation efficiency, expressed as the photosubstitution quantum yield (Φ). Previous research had shown that [Ru(tpy)(dmbpy)(SRR')]²⁺ complexes are less stable and more photoreactive than [Ru(tpy)(biq)(SRR')]²⁺ in water,^[14,17] thus preventing their application in PACT.^[18] In contrast, Turro et al. have demonstrated that complexes with L = pyridine are stable enough to be isolated while retaining photosubstitution properties under low-energy visible light ($\lambda_{\text{irr}} > 590 \text{ nm}$).^[12b,19] Here, the photoreactivity of **[1]Cl₂** and **[2]Cl₂** in water was tested under red-light irradiation. Figure 1 shows the evolution of the electronic absorption spectrum of **[1]**²⁺ upon activation at 625 nm under deoxygenated conditions in H₂O. The initial metal-to-ligand charge transfer (¹MLCT) band at 473 nm was gradually replaced by a new ¹MLCT band at $\lambda = 484 \text{ nm}$ with a clear isosbestic point at 477 nm, which indicates the formation of [Ru(tpy)(dmbpy)(H₂O)]²⁺ (*m/z* found 536.1, calc *m/z* 536.1 for [Ru(tpy)(dmbpy)(OH)]⁺). In the ¹H NMR spectra (Figure S2), under white-light irradiation in D₂O, the doublet for **[1]Cl₂** at 6.89 ppm was replaced by two doublets at 6.80 and 7.78 ppm, while the characteristic ¹Bu singlet at 0.94 ppm disappeared, thus confirming photodissociation of STF-31. The photosubstitution quantum yields (Φ_{625}) of 0.058 at RT and 0.080 at 37°C are consistent with thermal promotion of the triplet metal-centred states (³MC) from the photochemically generated ³MLCT states.^[12b] For **[2]Cl₂**, irradiation at 625 nm resulted in a shift of the MLCT band at 531 nm to 549 nm, and an aqua photoproduct [Ru(tpy)(biq)(H₂O)]²⁺ (found *m/z* = 607.8, calc *m/z* = 608.1 for [Ru(tpy)(biq)(OH)]⁺). The final spectrum for ¹H NMR in D₂O (Figure S3) showed a new, distinctive quartet at 8.86 ppm, and a decrease in the doublet at 6.69 ppm and singlet at 0.90 ppm. Photosubstitution occurred with a quantum yield Φ_{625} of 0.013 and

0.019 at RT and 37°C, respectively (Table 1). The lower photoreactivity of **[2]Cl₂** compared to **[1]Cl₂** is consistent with previous work.^[12b] Both **[1]Cl₂** ($\log P = -0.63 \pm 0.04$) and **[2]Cl₂** ($\log P = -0.08 \pm 0.04$, see the Supporting Information) are water-soluble, but STF-31 is not ($\log P = +3.92$), thus resulting in ligand precipitation during photosubstitution of STF-31 in the NMR tube. Hence the caging Ru complexes significantly increase the water solubility of the inhibitor. Before testing these compounds in cancer cells, the dose of red light necessary to obtain full activation in the cell irradiation setup was evaluated to be 20.6 J cm⁻², which corresponds to 10 minutes irradiation under normoxia (Figure S4).^[11]

Table 1: Absorption maxima (λ_{max}) and molar absorption coefficients at λ_{max} (ϵ) and at 625 nm (ϵ_{625}); photosubstitution quantum yields (Φ_{625}) at 298 and 310 K; ¹O₂ generation quantum yields (Φ^{Δ}) at 293 K; and photosubstitution reactivity ($\xi = \Phi_{625} \cdot \epsilon_{625}$).

Complex	λ_{max} in nm ^[a] [ϵ in M ⁻¹ cm ⁻¹]	ϵ_{625} ^[a] in M ⁻¹ cm ⁻¹	Φ_{625} ^[a] at 298 K (at 310 K)	Φ^{Δ} ^[b] at 293 K	ξ ^[20]
[1]Cl₂	473 (8050)	379	0.058 (0.080)	< 0.005	2.2 (3.0)
[2]Cl₂	531 (9320)	609	0.013 (0.019)	0.036	0.79 (1.2)

[a] In H₂O. [b] In CD₃OD.

The cytotoxicity of STF-31 and of its caged analogues **[1]Cl₂** and **[2]Cl₂** was first tested in normoxic conditions (21% O₂) against three human cancer cell lines (A549, MCF-7, and A431) and a non-cancerous cell-line (MRC-5).^[11] 24 h after seeding, the cells were treated with STF-31, **[1]Cl₂**, or **[2]Cl₂**, and after 6 hours incubation, one plate was irradiated with red light (628 nm, 20.6 J cm⁻²) while the other was left in the dark. At *t* = 48 h, medium was replaced. Cell viability was then assayed by using sulforhodamine B (SRB) 96 h after seeding.^[21] Half maximal effective concentrations (EC₅₀) for cell growth inhibition were calculated from the dose–response curves of treated vs. non-treated wells (Figure 2 and Table S1 in the Supporting Information).

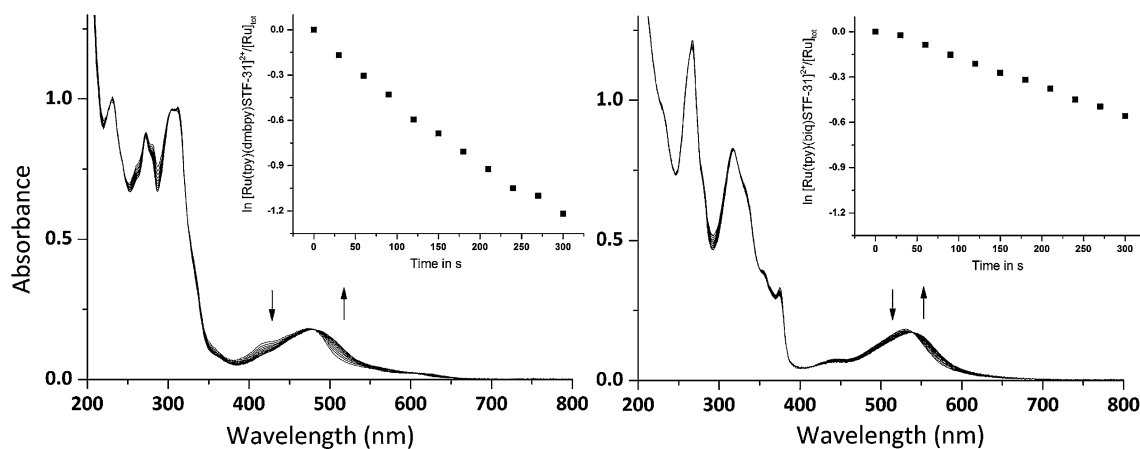


Figure 1. Electronic absorption spectra of **[1]Cl₂** (left) and **[2]Cl₂** (right) in deoxygenated H₂O under red-light irradiation (625 nm, photon flux 1.30 × 10⁻⁷ mol s⁻¹). *t*_{irr} = 5 min (every 30 s), *T* = 298 K.

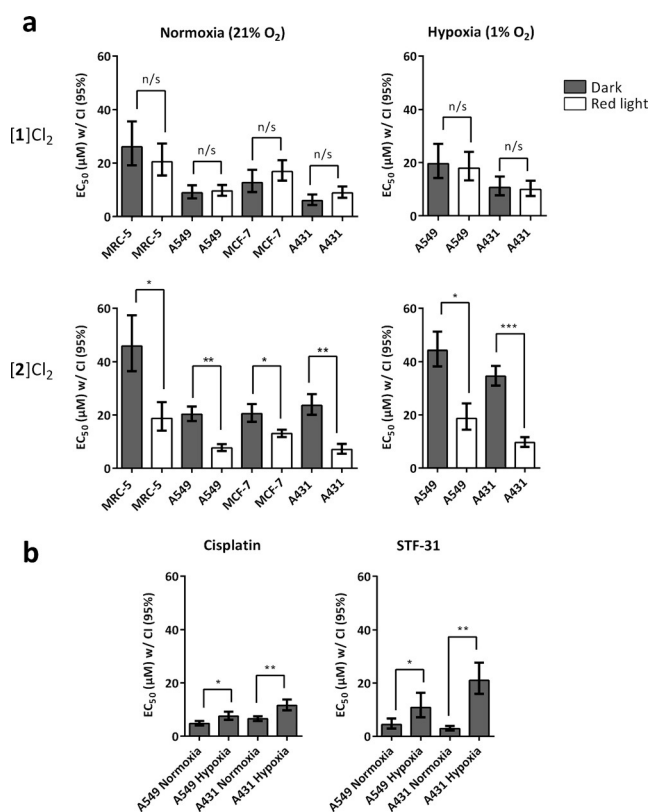


Figure 2. a) (Photo)cytotoxicity (EC_{50}) in μM for $[1]\text{Cl}_2$ and $[2]\text{Cl}_2$ in human cancer cells under normoxia and hypoxia. b) EC_{50} for STF-31 and cisplatin under normoxia and hypoxia (dark). Data points are averages ($n=3$) with 95% confidence intervals (in μM). * = $p \leq 0.05$, ** ≤ 0.01 , *** ≤ 0.001 . Also see Table S1.

Under normoxia (Figure 2a), STF-31 was highly cytotoxic in all of the cell lines, including MRC-5. $[1]\text{Cl}_2$ also showed substantial cytotoxicity in all of the cancerous cell lines, but its effect was limited in the non-cancerous MRC-5 cell line ($EC_{50} > 20 \mu\text{M}$). Importantly, a negligible difference was found between the irradiated and non-irradiated wells. This result was in great contrast to $[2]\text{Cl}_2$, which was less cytotoxic against the non-cancerous MRC-5 cells in the dark ($EC_{50} > 40 \mu\text{M}$) and highly toxic ($EC_{50} < 10 \mu\text{M}$) to cancerous cells after irradiation, with a marked difference in cytotoxicity between dark and irradiated cells for both A549 and A431 cells. Considering the minimal $^1\text{O}_2$ production efficiency (0.036, Table 1), this effect is most likely attributed to the anti-proliferative effect of the photoreleased STF-31.

To validate this hypothesis, $[1]\text{Cl}_2$, $[2]\text{Cl}_2$, and STF-31 were tested under hypoxia, in which $^1\text{O}_2$ generation is impaired. We therefore modified our published LED-based irradiation setup^[11] to allow irradiation of living cells while controlling the O_2 concentration (1.0–21%, Figure S7). We then repeated the cytotoxicity assay using the same protocol and light dose of 20.6 J cm^{-2} , but now at 1.0% O_2 (see Figure S7, lower left). As shown in Figure 2 and Table S1, the EC_{50} values for all of the compounds were found to be higher than under normoxia, which is consistent with earlier reports on the higher resistance of hypoxic cells to chemotherapy.^[22] No photocytotoxicity was observed for $[1]\text{Cl}_2$. However, the photo-

indices found for $[2]\text{Cl}_2$ under hypoxia (3.6 and 2.4 for A431 and A549) were identical to those found under normoxic conditions (3.3 and 2.6 for A431 and A549), thus demonstrating for the first time that a lower O_2 concentration does not affect the photoindex of the PACT compound $[2]\text{Cl}_2$.

We then investigated the enzyme-inhibition properties of STF-31, which is a reported GLUT-1 and NAMPT inhibitor.^[15a,16a,23] When GLUT-1-overexpressing A549 cells^[24] were starved using glucose-free medium, incubated for 2 h with a vehicle control (2% DMSO), 50 μM STF-31, or 100 μM phloretin (a well-known GLUT-1 inhibitor),^[25] and then treated with the fluorescent D-glucose analogue NBDG,^[26] and analysed by flow cytometry (Figure S10), STF-31 showed minimal glucose uptake inhibition compared to phloretin.^[27] Thus, the cytotoxicity of STF-31 is most likely not related to impaired glucose uptake and GLUT-1 inhibition.

The inhibitory effect of STF-31, $[1]\text{Cl}_2$, and $[2]\text{Cl}_2$ on NAMPT activity was then measured in recombinant NAMPT using the commercial Cyclex assay (Figure 3b). At 2 μM

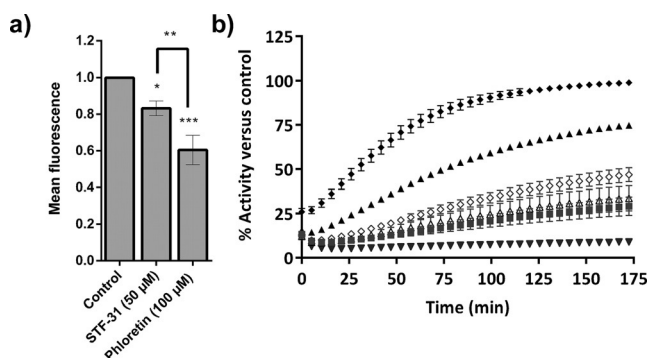


Figure 3. a) Normalized mean fluorescence intensity (MFI) of NBDG in A549 cells treated with control, STF-31, or phloretin. Data points are averages ($n=3$) \pm SD. * = $p \leq 0.05$, ** ≤ 0.01 , *** ≤ 0.001 . b) % of NAMPT activity observed for compounds vs. control (2% DMSO) after 1 h. Data points are averages ($n=2$) with \pm SEM. ● = Vehicle control, ◆ = $[2]\text{Cl}_2$ dark (2 μM), ▲ = $[1]\text{Cl}_2$ dark (2 μM), ◇ = $[2]\text{Cl}_2$ light (2 μM), △ = $[1]\text{Cl}_2$ light (2 μM), ■ = STF-31 (2 μM), ▼ = FK866 (20 μM).

concentration, STF-31 showed the largest effect on NAMPT activity, thus confirming that it is a NAMPT inhibitor.^[15a] $[2]\text{Cl}_2$ produced a dramatic reduction in NAMPT activity after red-light activation, whereas the non-irradiated sample showed much lower inhibition. A similar effect was observed for $[1]\text{Cl}_2$, although the dark activity was found to be much higher than for $[2]\text{Cl}_2$. The dark half maximal inhibitory concentrations (IC_{50}) of 4.8 μM for $[2]\text{Cl}_2$ was lowered by a factor of 18 down to 0.26 μM after irradiation, which is similar to the value obtained for STF-31 (0.25 μM , Table 2). The NAMPT inhibitory effect of STF-31 was thus fully recovered upon red-light activation of $[2]\text{Cl}_2$.

The almost identical EC_{50} found for $[1]\text{Cl}_2$ in the dark and after light irradiation, and its high NAMPT inhibition in the dark, suggest that $[1]\text{Cl}$ is thermally unstable: When followed for 48 hours at 37 $^{\circ}\text{C}$ in the dark in OptiMEM medium (Figure S8), $[1]^{2+}$ slowly decomposed to $[\text{Ru}(\text{tpy})(\text{dmbpy})-(\text{OH})_2]^{2+}$ while $[2]^{2+}$ remained stable (Figure 4 and Fig-

Table 2: NAMPT activity inhibitory concentration (IC_{50} with 95% confidence intervals, in μM) obtained for STF-31 and $[2]\text{Cl}_2$ in the dark and $[2]\text{Cl}_2$ after red-light irradiation.^[a]

STF-31		$[2]\text{Cl}_2$				
IC_{50} μM (Dark)	CI ^[b]	IC_{50} μM (Dark)	CI ^[b]	IC_{50} μM (625 nm)	PI ^[c]	
0.25	+0.027 −0.027	4.8	+0.89 −0.75	0.26	+0.079 −0.094	18

[a] Samples were irradiated for 10 minutes at 37°C. See the Supporting Information. [b] Confidence interval. [c] Photoindex (PI) = $IC_{50,\text{dark}}/IC_{50,\text{light}}$.

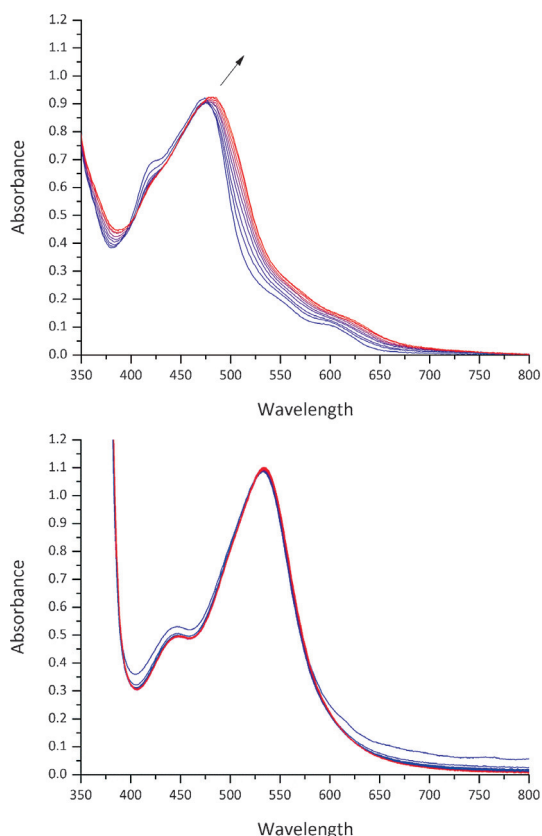


Figure 4. Stability of $[1]\text{Cl}_2$ (top) and $[2]\text{Cl}_2$ (bottom) in OMEM media + 2.5% fetal calf serum (FCS) at 37°C over 48 hours in the dark. Spectra measured each hour, the blue spectra were measured first, the red ones last. Arrow (top) indicates a shift of the MLCT absorption maximum due to formation of the chlorido species.

ure S9). This result is in contrast to Kodanko et al., who used $[\text{Ru}(\text{tpy})(\text{dmbpy})]^{2+}$ to cage a steroidal CYP17A1 inhibitor.^[12a] According to our results, $[\text{Ru}(\text{tpy})(\text{NN})(\text{L})]^{2+}$ complexes are only stable enough for PACT when NN = biq, while complexes with NN = dmbpy are more photoreactive and are also unstable in the dark.^[14]

In conclusion, we have demonstrated for the first time the potential of PACT in hypoxic cancer cells using a photocaged NAMPT inhibitor. Whereas under hypoxic conditions, classical type II PDT would not be effective because of the absence of oxygen, $[2]\text{Cl}_2$ represents a promising form of

photocaged drug, with a similar photoindex under hypoxia (1% O_2) compared to normoxia (21% O_2). Also, this compound is soluble in water and activated using red light, whereas most PACT compounds reported to date require UV, blue or green light for activation. The steric hindrance of $[2]\text{Cl}_2$ is high enough to obtain activation using clinically relevant red-light doses (21 J cm^{-2}),^[28] but low enough to maintain thermal stability. In contrast, $[1]\text{Cl}_2$ is too labile in the dark, which make it unsuitable for PACT. Altogether this study represents the first example of PACT where the phototoxicity index measured in hypoxic cancer cells with red light can be explained by a low $^1\text{O}_2$ quantum yield, an efficient oxygen-independent photosubstitution reaction, and enzyme inhibition.

Acknowledgements

This work was supported by the Dutch Organization for Scientific Research (NWO-CW) through a VIDI grant to S.B. The European Research Council is acknowledged for financial support through a Starting Grant to S.B. Prof. Elisabeth Bouwman is kindly acknowledged for scientific support and input. Dr. Bart Limburg is kindly acknowledged for setting up the irradiation setup for UV/Vis experiments. Hans den Dulk is kindly acknowledged for help with setting up the hypoxic incubator. Gerwin Spijksma and Hans van den Elst are kindly acknowledged for measuring HRMS samples.

Conflict of interest

The authors declare no conflict of interest.

Keywords: anti-tumor agents · hypoxia · photopharmacology · red-light activation · ruthenium

How to cite: *Angew. Chem. Int. Ed.* **2017**, *56*, 11549–11553
Angew. Chem. **2017**, *129*, 11707–11711

- [1] A. D. Gujar, S. Le, D. D. Mao, D. Y. Dadey, A. Turski, Y. Sasaki, D. Aum, J. Luo, S. Dahiya, L. Yuan, K. M. Rich, J. Milbrandt, D. E. Hallahan, H. Yano, D. D. Tran, A. H. Kim, *Proc. Natl. Acad. Sci. USA* **2016**, *113*, E8247–E8256.
- [2] a) J. A. Khan, X. Tao, L. Tong, *Nat. Struct. Mol. Biol.* **2006**, *13*, 582–588; b) C. A. Lyssiotis, L. C. Cantley, *Clin. Cancer Res.* **2014**, *20*, 6–8.
- [3] B. Tan, D. A. Young, Z. H. Lu, T. Wang, T. I. Meier, R. L. Shepard, K. Roth, Y. Zhai, K. Huss, M. S. Kuo, J. Gillig, S. Parthasarathy, T. P. Burkholder, M. C. Smith, S. Geeganage, G. Zhao, *J. Biol. Chem.* **2013**, *288*, 3500–3511.
- [4] T. S. Zabka, J. Singh, P. Dhawan, B. M. Liederer, J. Oeh, M. A. Kauss, Y. Xiao, M. Zak, T. Lin, B. McCray, N. La, T. Nguyen, J. Beyer, C. Farman, H. Uppal, P. S. Dragovich, T. O'Brien, D. Sampath, D. L. Misner, *Toxicol. Sci.* **2015**, *144*, 163–172.
- [5] a) D. Crespy, K. Landfester, U. S. Schubert, A. Schiller, *Chem. Commun.* **2010**, *46*, 6651–6662; b) C. Mari, V. Pierroz, S. Ferrari, G. Gasser, *Chem. Sci.* **2015**, *6*, 2660–2686; c) U. Schatzschneider, *Eur. J. Inorg. Chem.* **2010**, 1451–1467; d) N. J. Farrer, L. Salassa, P. J. Sadler, *Dalton Trans.* **2009**, 10690–10701; e) A. Presa, R. F. Brissos, A. B. Caballero, I. Borilovic, L. Korrodi-Gregório, R.

- Pérez-Tomás, O. Roubeau, P. Gamez, *Angew. Chem. Int. Ed.* **2015**, *54*, 4561–4565; *Angew. Chem.* **2015**, *127*, 4644–4648.
- [6] T. Respondek, R. Sharma, M. K. Herroon, R. N. Garner, J. D. Knoll, E. Cueny, C. Turro, I. Podgorski, J. J. Kodanko, *Chem-MedChem* **2014**, *9*, 1306–1315.
- [7] a) E. M. Rial Verde, L. Zayat, R. Etchenique, R. Yuste, *Front. Neural Circuits* **2008**, *2*, 2; b) B. S. Howerton, D. K. Heidary, E. C. Glazer, *J. Am. Chem. Soc.* **2012**, *134*, 8324–8327; c) S. Betanzos-Lara, L. Salassa, A. Habtemariam, O. Novakova, A. M. Pizarro, G. J. Clarkson, B. Liskova, V. Brabec, P. J. Sadler, *Organometallics* **2012**, *31*, 3466–3479; d) A. Habtemariam, C. Garino, E. Ruggiero, S. Alonso-de Castro, J. Mareque Rivas, L. Salassa, *Molecules* **2015**, *20*, 7276–7291.
- [8] a) P. Anstaett, V. Pierroz, S. Ferrari, G. Gasser, *Photochem. Photobiol. Sci.* **2015**, *14*, 1821–1825; b) L. Zayat, M. G. Noval, J. Campi, C. I. Calero, D. J. Calvo, R. Etchenique, *ChemBioChem* **2007**, *8*, 2035–2038; c) T. Joshi, V. Pierroz, C. Mari, L. Gemperle, S. Ferrari, G. Gasser, *Angew. Chem. Int. Ed.* **2014**, *53*, 2960–2963; *Angew. Chem.* **2014**, *126*, 3004–3007.
- [9] D. E. Dolmans, D. Fukumura, R. K. Jain, *Nat. Rev. Cancer* **2003**, *3*, 380–387.
- [10] P. Avci, A. Gupta, M. Sadasivam, D. Vecchio, Z. Pam, N. Pam, M. R. Hamblin, *Semin. Cutaneous Med. Surg.* **2013**, *32*, 41–52.
- [11] S. L. Hopkins, B. Siewert, S. H. Askes, P. Veldhuizen, R. Zwier, M. Heger, S. Bonnet, *Photochem. Photobiol. Sci.* **2016**, *15*, 644–653.
- [12] a) A. Li, R. Yadav, J. K. White, M. K. Herroon, B. P. Callahan, I. Podgorski, C. Turro, E. E. Scott, J. J. Kodanko, *Chem. Commun.* **2017**, *53*, 3673–3676; b) J. D. Knoll, B. A. Albani, C. B. Durr, C. Turro, *J. Phys. Chem. A* **2014**, *118*, 10603–10610; c) J. D. Knoll, B. A. Albani, C. Turro, *Acc. Chem. Res.* **2015**, *48*, 2280–2287.
- [13] H. Yin, M. Stephenson, J. Gibson, E. Sampson, G. Shi, T. Sainuddin, S. Monro, S. A. McFarland, *Inorg. Chem.* **2014**, *53*, 4548–4559.
- [14] A. Bahreman, B. Limburg, M. A. Siegler, E. Bouwman, S. Bonnet, *Inorg. Chem.* **2013**, *52*, 9456–9469.
- [15] a) D. J. Adams, D. Ito, M. G. Rees, B. Seashore-Ludlow, X. Puyang, A. H. Ramos, J. H. Cheah, P. A. Clemons, M. Warmuth, P. Zhu, A. F. Shamji, S. L. Schreiber, *ACS Chem. Biol.* **2014**, *9*, 2247–2254; b) P. S. Dragovich, K. W. Bair, T. Baumeister, Y. C. Ho, B. M. Liederer, X. Liu, Y. Liu, T. O'Brien, J. Oeh, D. Sampath, N. Skelton, L. Wang, W. Wang, H. Wu, Y. Xiao, P. W. Yuen, M. Zak, L. Zhang, X. Zheng, *Bioorg. Med. Chem. Lett.* **2013**, *23*, 4875–4885; c) E. M. Kropp, B. J. Oleson, K. A. Broniowska, S. Bhattacharya, A. C. Chadwick, A. R. Diers, Q. Hu, D. Sahoo, N. Hogg, K. R. Boheler, J. A. Corbett, R. L. Gundry, *Stem Cells Transl. Med.* **2015**, *4*, 483–493.
- [16] a) D. A. Chan, P. D. Sutphin, P. Nguyen, S. Turcotte, E. W. Lai, A. Banh, G. E. Reynolds, J. T. Chi, J. Wu, D. E. Solow-Cordero, M. Bonnet, J. U. Flanagan, D. M. Bouley, E. E. Graves, W. A. Denny, M. P. Hay, A. J. Giaccia, *Sci. Transl. Med.* **2011**, *3*, 94ra70; b) M. Bonnet, J. U. Flanagan, D. A. Chan, A. J. Giaccia, M. P. Hay, *Bioorg. Med. Chem.* **2014**, *22*, 711–720; c) D. Kraus, J. Reckenbeil, M. Wenghoefer, H. Stark, M. Frentzen, J. P. Allam, N. Novak, S. Frede, W. Gotz, R. Probstmeier, R. Meyer, J. Winter, *Cell. Mol. Life Sci.* **2016**, *73*, 1287–1299.
- [17] A. J. Göttle, F. Alary, M. Boggio-Pasqua, I. M. Dixon, J. L. Heully, A. Bahreman, S. H. Askes, S. Bonnet, *Inorg. Chem.* **2016**, *55*, 4448–4456.
- [18] See Ref. [14].
- [19] See Ref. [12b].
- [20] A. Bahreman, J. A. Cuello-Garibo, S. Bonnet, *Dalton Trans.* **2014**, *43*, 4494–4505.
- [21] V. Vichai, K. Kirtikara, *Nat. Protoc.* **2006**, *1*, 1112–1116.
- [22] J. P. Cosse, C. Michiels, *Anti-Cancer Agents Med. Chem.* **2008**, *8*, 790–797.
- [23] a) C. Xintaropoulou, C. Ward, A. Wise, H. Marston, A. Turnbull, S. P. Langdon, *Oncotarget* **2015**, *6*, 25677–25695; b) T. Matsumoto, S. Jimi, K. Migita, Y. Takamatsu, S. Hara, *Leuk. Res.* **2016**, *41*, 103–110.
- [24] J. Park, H. Y. Lee, M. H. Cho, S. B. Park, *Angew. Chem. Int. Ed.* **2007**, *46*, 2018–2022; *Angew. Chem.* **2007**, *119*, 2064–2068.
- [25] S. C. Hsu, R. S. Molday, *J. Biol. Chem.* **1991**, *266*, 21745–21752.
- [26] C. Zou, Y. Wang, Z. Shen, *J. Biochem. Biophys. Methods* **2005**, *64*, 207–215.
- [27] L. Ma, R. Wang, Y. Nan, W. Li, Q. Wang, F. Jin, *Int. J. Oncol.* **2016**, *48*, 843–853.
- [28] S. S. Dhillon, T. L. Demmy, S. Yendamuri, G. Loewen, C. Nwogu, M. Cooper, B. W. Henderson, *J. Thorac. Oncol.* **2016**, *11*, 234–241.

Manuscript received: April 19, 2017

Revised manuscript received: June 12, 2017

Accepted manuscript online: June 30, 2017

Version of record online: August 9, 2017